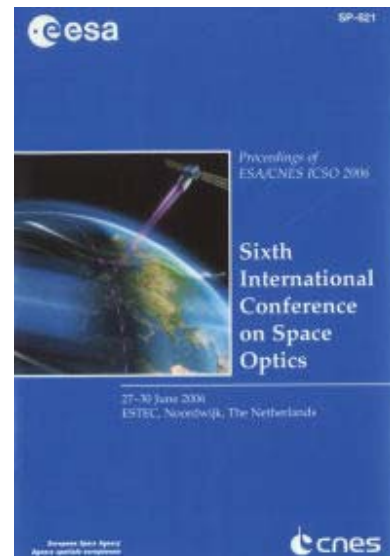


# International Conference on Space Optics—ICSO 2006

Noordwijk, Netherlands

27–30 June 2006

*Edited by Errico Armandillo, Josiane Costeraste, and Nikos Karafolas*



## *DARWIN system concepts*

*Oswald Wallner, Klaus Ergenzinger, Reinhold Flatscher,  
Ulrich Johann*



## DARWIN SYSTEM CONCEPTS

Oswald Wallner, Klaus Ergenzinger, Reinhold Flatscher, and Ulrich Johann

EADS Astrium GmbH, 88039 Friedrichshafen, Germany

### ABSTRACT

The European DARWIN mission aims at the detection of Earth-like exo-planets and at the spectroscopic characterization of their atmospheres. By nulling interferometry in the mid-infrared wavelength regime the stellar flux may be rejected. By spatial and temporal modulation of the interferometer's receive characteristic the planet signal may be extracted from the background signals. The DARWIN instrument consists of a flotilla of free-flying spacecraft, three to four spacecraft carrying the collector telescopes and one spacecraft carrying the control units and the beam recombination and detection unit. We present different system design concepts for the DARWIN instrument which have been elaborated within the DARWIN System Assessment Study. We discuss various aperture configurations and beam routing schemes as well as modulation methods and beam recombination schemes.

### 1. INTRODUCTION

With the DARWIN [1] mission the European Space Agency plans to find and investigate Earth-like exoplanets orbiting Sun-like stars. By spectroscopic analysis of the received planet light the presence of absorption features shall give hints on biological activity and, in further consequence, on life similar to that evolved on Earth. The envisaged biomarkers water, ozone, methane or carbon-dioxide determine the operational wavelength range in the mid-infrared.

The method to be applied is nulling interferometry [2], a technique providing high on-axis light suppression and high angular resolution due to the strong dependence of the transmission on the light's angle of incidence resulting from a large baseline. In the simplest arrangement of a nulling interferometer, the sum of star and planet light is received by several identical telescopes. The optical path lengths from the telescopes to the recombination unit are set so that the on-axis star signal experiences destructive interference. The star light is strongly suppressed by the central null of the interferometer's receive characteristic,

while the planet light experiences constructive interference by proper adjustment of the baseline.

In view of the actual implementation of the DARWIN mission we have evaluated several options and alternatives which shall guarantee optimum science return. After an overview over the DARWIN mission, we discuss the different mission options and identify the optimum solutions. We present the results of the science performance simulations for the most promising configurations. These and the assessment of complexity, cost and risk lead us to a proposal for a baseline concept for the DARWIN mission.

### 2. THE DARWIN MISSION

The DARWIN instrument is a space-borne nulling interferometer operating in the mid-infrared from 6.5 to 20  $\mu\text{m}$  wavelength. The instrument is distributed over several spacecraft which fly in a closely-controlled formation. In this way the interferometer is formed by its distributed optical components.

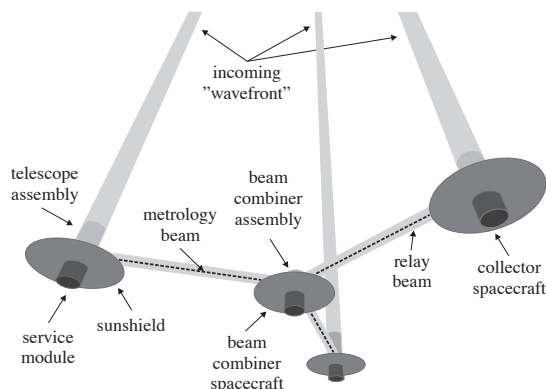


Figure 1. DARWIN interferometer configuration showing the distributed payload on the collector spacecraft and on the beam combiner spacecraft, respectively, in science mode formation flying.

The formation control functionality is based on hardware distributed among the payload assemblies of all space-

craft and partially residing in the service modules. Besides aligning the spacecraft and maintaining the spacecraft positions, the formation control system performs the resizing and rearranging of the formation as well as array rotation during science operation. Compared to a physical structure the formation flying system has the advantage of easy reconfiguration and of better control of the incoming signals for large interferometric arm lengths. The distances between the collector telescopes are adjustable and range from some tens to some hundreds of meters. Figure 1 shows the DARWIN interferometer configuration, i.e. the distributed payload on the collector spacecraft and on the beam combiner spacecraft, respectively, in science mode formation flying.

### 3. DARWIN MISSION AND CONFIGURATION OPTIONS

For an optimum implementation of the DARWIN mission which allows for maximum science return, we have traded off options and alternatives for several mission aspects. In the following we review that mission options which have the most critical impact on the science performance and provide recommendations for their implementation.

#### 3.1. Aperture Configurations

The aperture configuration, i.e. the arrangement of the receive telescopes relative to each other, determines together with the relative phase differences between the received signals the angular receive characteristic of the DARWIN nulling interferometer. Identical optical path lengths from the receive telescopes to the beam recombination unit and achromatic phase shifter result in destructive interference for the on-axis star signal. Depending on the actual aperture configuration the off-axis signals experience interference due to optical path length differences. The aperture configuration therefore determines the off-axis receive characteristic of the DARWIN interferometer. Besides the scientific performance the choice of the aperture configuration is driven by technical limitations. Mass, volume, and cost constraints for the launcher limit the total number of collector spacecraft to four because a reasonably large collecting area is required to achieve the science requirements. For removal of noise sources as spurious background signals, drifts, and some types of instability noise, at least three aperture configurations are required as these allow for phase chopping. Aperture configurations with a null depth proportional to the square of the off-axis angle  $\Theta$  are preferred as they yield a higher planet detection signal-to-noise ratio (SNR) compared to  $\Theta^4$ -configurations. For minimizing the effect of stray light the collector spacecraft have to be arranged in one plane. This imposes constraints on the spacecraft separation as the minimum spacing shall not be smaller than 5 meters. For achieving deep nulling

of the star, aperture configurations and instrument concepts are mandatory which results in beams with identical transverse field distribution, equal state of polarization, and proper phase relation.

The first row of Tab. 1 shows the aperture configurations and angular receive characteristics for the different three and four telescope formations investigated which all fulfill the criteria mentioned above but show different science performance. The three telescope nullers [3] (TTN) can be realized as linear, orthogonal or triangular arrays. The triangular TTN shows a  $120^\circ$  degree symmetry of the receive characteristic therefore does not allow for unambiguous planet detection. The four aperture configurations may be realized by the combination of two two-telescope nullers. This means for the dual-chopped Bracewell [4] (DCB) configuration that an instrument with low or high angular resolution is possible. However, high resolution goes hand in hand with low star light suppression, while high suppression of stellar leakage causes low resolution. The x-Array [5] allows for decoupling of the nulling and the imaging properties. By arranging the telescopes to form a rectangle and by proper recombination the nulling baseline  $B$  is independent from the imaging baseline  $X_B B$ .

All aperture configurations in Tab. 1 show a central null  $N$  which is proportional to the square of the off-axis angle  $\Theta$ ,  $N \propto (\pi B \Theta / \lambda)^2$ , where  $B$  is the interferometer array's baseline, defined as the smallest center-to-center distance between two collector spacecraft telescopes. For a single wavelength  $\lambda$  the optimum baseline – which results in constructive interference for the planet signal – is given by  $B = (\alpha/n) \cdot (\lambda/B)$ , where  $\alpha/n$  is a proportionality factor determined by the exact aperture configuration and  $n$  is the number of apertures. In practice the optimum baseline is the result of an optimization procedure because of the wide operational wavelength range from 6.5 to  $20\mu m$  and the uncertainty of the actual planet position in detection mode. For some nearby F-class stars this optimum baseline cannot be realized due to safe formation flying constraints.

#### 3.2. Spacecraft Formation and Beam Routing

The DARWIN payload is distributed over the free-flying spacecraft of the formation. Due to stray light reasons, the collector spacecraft have to be arranged in one plane. The beam combiner spacecraft may be located in the same plane, leading to a planar formation, or above the plane of the collector spacecraft, leading to a non-planar formation. The latter is sometimes denoted as “EMMA”. In the planar case the incoming light is received by the telescopes of the collector spacecraft and is routed by the relay optics towards the beam combiner spacecraft. In the non-planar case the incoming light is reflected by the large mirrors of the collector spacecraft and is focussed onto the receive optics of the beam combiner spacecraft which is located about 1000 meters above the plane of the collector spacecraft. The mirrors represent sections

of a virtual parabola which are approximated by spherical mirrors to better adapt to different baselines. All aperture configurations discussed in Sec. 3.1 can be realized as planar or non-planar spacecraft formations.

The non-planar spacecraft formations have the advantage that a larger number of stars is accessible. While the planar constellations are limited to ecliptic latitudes of  $\pm 45^\circ$ , the non-planar formations can access a region of  $\pm 72^\circ$ , which corresponds to 36% more targets from the DARWIN target catalogue [6]. This advantage comes at the cost of severe instrumental difficulties. To allow for deep nulling, a perfectly symmetric beam routing scheme is required which does not change the state of polarization between the individual beams and which does not introduce intensity or phase differences. The beam routing further has to ensure equal optical path lengths from the individual telescopes to the beam recombination unit. For the planar spacecraft formations these requirements can be fulfilled by proper design because the beams are routed in one plane. The beam routing schemes for the non-planar formations are inherently asymmetric with respect to polarization. While this effect is negligible for small baselines, it has a serious impact for larger baselines. The non-planar formations require a complicated cryogenic beam derotation optics as the beam combiner spacecraft has to remain fixed relative to the Sun when the array is rotated. Further they require a huge corrector to compensate the unavoidable wavefront aberrations caused by the off-axis spherical mirror reflections. Compared to the perfectly symmetric and well established concepts for the planar formations, the non-planar formations inherently suffer from inferior instrumental performance and would require a huge effort for developing new instrument concepts. Especially on ground qualification of long focal length optics (1000 meters) is very demanding and highly critical.

A challenge for the DARWIN mission where several spacecraft fly in a close formation is the control of stray light. For a rough order of magnitude estimation we assumed that by proper design no stray light can be coupled directly into the single-mode fiber but is scattered by the first mirror of the beam combiner spacecraft receive optics. The major sources of stray light are thermal emission and specular reflection from the collector spacecraft sunshields as well as scattering and diffraction at all sunshields. The non-planar formations have an intrinsic advantage as the beam combiner spacecraft is far away (typically 1000 meters) from the collector spacecraft and further can only see the cold side of the sunshields. However, the small single-mode fiber etendue together with proper design of the baffles and the multi-layer sunshields allows for rejection of stray light to acceptable levels also for planar formations. This holds also for the thermal emission from the sunshields in case of large baselines where the baffling can be further relieved by raising the relay beam as high as possible above the collector spacecraft sunshield.

### 3.3. Interferometer Implementation

The DARWIN interferometer basically consists of the modulation unit and the beam recombination unit. By modulating the telescope array instead of using a static configuration the vulnerability to spurious effects is reduced and the planet localization capability is improved. Two types of modulation are applied, phase chopping and array rotation.

Phase chopping is achieved by two sub-interferometers which are recombined with variable phase shifts. The required conjugated receive characteristics can only be realized with aperture configurations as shown in Tab. 1 which have fractional  $\pi$  phase shifts between the individual beams. Phase chopping has the advantage to compensate for any uniform background noise, for drifts in the nulling performance or detector performance, and for some instability noise [7] contributors. The two conjugated receive characteristics can either be realized sequentially by actuating the achromatic phase shifters or concurrently by splitting the set of input beams into two subsets of beams. To each subset the phase shifts corresponding to the respective chop state are applied and the beams are switched by proper optics. The latter is clearly preferable as it increases the available observation time and avoids complex actuation mechanisms. For the three and four aperture configurations modulation schemes are possible which allow for efficient phase chopping. The second row of Tab. 1 shows the modulation maps resulting from phase chopping. For the three telescope nullers the maximum of the modulation map amounts to  $N_{\max} = 70\%$ , taking into account an efficiency of 75% for beam recombination. For the four aperture configurations a maximum of  $N_{\max} = 100\%$  is possible because the instrument is realized by two two-telescope nullers. In both cases the bulk transmission has not been taken into account.

Continuous rotation of the telescope array around the array's line of sight results in a temporally varying receive characteristic of the DARWIN instrument and therefore in a temporal modulation of the detected signals. Because the transmission of centro-symmetric sources is not affected, the planet signal can be discriminated from all other signals. Depending on the receive characteristic, i.e. on the actual aperture configuration, and depending on the planet location, different signals are obtained by rotating the array. The third row of Tab. 1 shows the modulation maps resulting from array rotation. The rotational modulation efficiency is a measure how efficiently a planet is modulated by a certain aperture configuration. It is defined as the mean over all possible angular planet positions of the root-mean-square (rms) modulation for one full rotation round the array's line of sight. The linear aperture configurations show highest modulation efficiency because they have a rather uniform modulation behavior over the entire field of view. Due to the high angular resolution, the x-Array shows a high frequency modulation of the off-axis planet signal. By applying correlation methods, the DARWIN instrument allows for

source scene reconstruction. The fourth row of Tab. 1 shows the correlation maps which results from the correlation of a planet signal with the signals from all possible planet locations within the field of view. Unambiguous and reliable reconstruction can be expected if a single and sharp correlation maximum occurs and if all sidelobes are weak compared to the main peak. The width of the corre-

lation peak is quantified by its full-width-half-maximum (FWHM), i.e. by the geometric mean of the FWHM in radial and azimuthal direction. That fraction  $F_{corr}$  of the field of view where the correlation exceeds 50% allows to evaluate the influence of the sidelobes. The orthogonal TTN and in particular the x-Array clearly show the best performance concerning reconstruction.

	linear TTN	orthogonal TTN	triangular TTN	DCB	x-Array (3:1)
configuration					
receive charact.					
phase chopping					
array rotation					
reconstruction					
	$M_{max} = 70\%$	$M_{max} = 70\%$	$M_{max} = 70\%$	$M_{max} = 100\%$	$M_{max} = 100\%$
	$\eta = 24.3\%$	$\eta = 19.5\%$	$\eta = 17.9\%$	$\eta = 34.9\%$	$\eta = 28.8\%$
	FWHM = 317mas $F_{corr} = 5.8\%$	FWHM = 86mas $F_{corr} = 1.0\%$	FWHM = 72mas $F_{corr} = 4.3\%$	FWHM = 350mas $F_{corr} = 5.6\%$	FWHM = 38mas $F_{corr} = 0.8\%$

Table 1. Modulation and reconstruction characteristics for three and four aperture configurations. The first row shows the modulation maps resulting from phase chopping ( $M_{max}$  is the maximum value), the second row shows the modulation maps resulting from array rotation in polar coordinates ( $\eta$  is the modulation efficiency), and the third row shows the correlation maps resulting from reconstruction (FWHM is the full-width-half-maximum of the main peak and  $F_{corr}$  is the fraction of the field of view where the correlation exceeds 50%).

The beam recombination can be done either in the pupil plane by a co-axial scheme realized in bulk optics or in the image plane by coupling the beams multi-axially into a single-mode fiber [8]. For DARWIN the beam recombination subsystem has to be very efficient with respect to optical throughput and has to be perfectly symmetric, i.e. no differential effects with respect to the transverse distribution of amplitude and phase and with respect to the state of polarization may be introduced. Because of the asymmetry between the two output beams, pupil plane recombination with dielectric beam splitters has to be realized by a symmetrizing double path structure [9]. The resulting beam recombination schemes are perfectly symmetric and have a theoretical efficiency of 100% for four beams and an efficiency of 75% for three beams. For image plane recombination the parallel beams are coupled off axis into the single-mode fiber. For a practical setup this results in a clearly reduced coupling efficiency and in non-negligible differential polarization effects. The main drawback of image plane recombination is the sensitivity to misalignment which is by one order of magnitude more severe compared to pupil plane recombination. Pupil plane recombination with bulk optics clearly outperforms image plane recombination in terms of symmetry (i.e. nulling performance) and efficiency.

### 3.4. Launch Vehicle and Accommodation

Single and dual launch scenarios have been envisaged for DARWIN. While a single launch imposes constraints on the available mass and volume, two launchers cause additional cost and significantly increase the mission complexity due to the required rendezvous in space. Launch with two Soyuz-ST Fregats has been abandoned as it is not compatible with the mass and volume requirements. A single launch scenario with an Ariane 5 launcher is therefore the only reasonable option for the DARWIN mission.

The Ariane 5 ECA launcher with long fairing has a maximum payload envelope of about 4.5 meters diameter and a launch capacity of about 7000 kilograms for a DARWIN-representative direct injection scenario. The primary driver for the launch configuration is the size of the collector telescope as it determines the overall mass and volume of the launch composite. The baseline for our design is a diameter of 3.15 meters for the telescope's primary mirror but diameters up to 3.5 meters can be safely accommodated. The remaining volume is, e.g., required for stowing the sunshields and for the load-carrying structure used for stacking several spacecraft within the launch vehicle fairing.

Launch with the Ariane 5 ECA launcher is only constrained by the volume available for accommodation. The spacecraft for non-planar formations can be easily accommodated as the collector spacecraft only carry reflecting mirrors. For planar formations, the limited launch volume requires deployable secondary mirrors for collector telescopes of reasonable size. This necessitates

a stable deployment mechanism and additional metrology for accurate positioning.

### 3.5. Transfer and Operational Orbit

Launch to the operational orbit is either done by direct injection into a transfer to L2 or by injection from a highly eccentric Earth orbit by applying apogee-raising propulsion. While the latter option only allows for the transfer of the entire spacecraft stack, direct injection also allows for early spacecraft separation and individual transfer. Apogee raising propulsion is not the preferred option as it requires additional stack operational modes and additional spacecraft functionality on the propulsion module.

Separation of the spacecraft can be done in LEOP (launch and early orbit phase) or at L2. Separation at L2 has the drawback that it is a non-usual procedure in a non-usual environment and that the assembled spacecraft stack has to be engineered, tested and operated in addition to the individual spacecraft. The advantage of separation in LEOP is that during cruise the spacecraft can be initialized and the metrology can be commissioned. Direct injection and early deployment in LEOP therefore is the preferred transfer and separation strategy. For the required dispersion correction either dedicated chemical propulsion modules or solar electric propulsion can be used. The first has the advantage of high reliability and low cost, but the drawback of increased testing, necessity of flushing or separating the propulsion tanks, and additional operational modes. Solar electric propulsion is the preferred option because it allows for combination of the dispersion correction with the formation flying coarse control.

A Halo orbit at L2 is the preferred option for DARWIN as it allows for simplified operations compared to a Lissajous orbit. The latter experiences eclipses and shows a variable Earth contact geometry. Free insertion Halo orbits can be reached by Ariane 5 from the Guiana Space Center in Kourou for approximately half a year and only small insertion manoeuvres are required for the rest of the year. The insertion manoeuvres can be performed by the solar electric propulsion which is also used for dispersion correction and formation coarse control.

## 4. SCIENCE PERFORMANCE

To evaluate the science performance of the different aperture configurations we calculated for each target of the DARWIN prime target catalogues [6] the integration time required to achieve a specified SNR for detection and for spectroscopy of the demodulated planet signal. We analyzed the most promising three and four aperture configurations, namely the orthogonal TTN with planar and non-planar spacecraft formation and the planar x-Array with an imaging to nulling baseline ratio of  $X_B = 3$ . During the nominal mission lifetime of 5 years the DARWIN

mission shall be capable of detecting 225 planets assuming an exo-zodi level corresponding to that of the Earth (1 zodi) and of 150 planets for ten times stronger dust clouds (10 zodi). It shall further be capable of spectroscopically characterizing at least 22 or 15 planets during the nominal mission lifetime, assuming 1 or 10 zodi, respectively.

For each aperture configuration we optimized the interferometer baseline for all targets to allow for optimum observation performance. Because the actual planet position is a priori unknown, we assume a probability distribution for the apparent distance of the planet from the parent star which is determined by uniform distributions for the radius of the circular orbit ranging from 0.7 – 1.5 times the habitable distance, for the orbit inclination from 0 to  $\pi/2$ , and for the orbital phase from 0 to  $2\pi$ . For each target the demodulated planet signal is calculated for a range of possible positions to allow for a detection probability of 90%. Each planet is observed 3 times to be able to determine the orbit parameters. For planet detection the signal within the entire observation band from 6.5 to  $20\mu m$  is integrated to achieve a SNR of 5 for 90% detection probability. We applied the method of rotating spectroscopy as it allows for improved performance compared to staring spectroscopy. For spectroscopy the SNR requirements follow from the accuracy with which the flux absorbed by the atmospheric features has to be measured. For the required SNR on the nominal black-body continuum, we underlayed for methane a value of 8.8, for ozone a value of 15.6, for carbon-dioxide a value of 13.3, and for water a value of 10 at the lower edge and of 30 at the upper wavelength band edge. For the simulation we applied a frequency domain approach [7] which allows for taking into account instability noise. For the amplitude and the optical path difference (OPD) perturbations we assumed a  $1/f$  power spectrum with a cutoff frequency of  $10kHz$  and a rms value of 0.035% and  $1nm$ , respectively. For the instrument we assumed a realistic implementation with typical parameters for all devices and sub-systems. To allow for sufficient throughput, the observational wavelength band has been split into two subbands. We assumed for the observation procedure a duty cycle of 70% and assessed whether the mission goals can be fulfilled by analyzing how many targets can be detected and spectroscopically characterized within the nominal mission lifetime.

Figure 2 shows for promising formations the number of detected targets as a function of the observation time. Concerning planet detection all formations are compliant with the mission requirements of searching 225 or 150 targets for 1 or 10 zodi, respectively. The x-Array clearly outperforms all other configurations because of its higher efficiency, caused by the larger collecting area and the more efficient modulation and recombination stage. For the orthogonal TTN the non-planar spacecraft formation shows better performance compared to the planar formation because a larger number of targets is accessible which also show advantageous detection properties. However, the unavoidable performance degradation for the non-planar formations, e.g. due to differential polarization effects, has not been taken into account.

Whether the different formations are compliant with the requirements concerning planet characterization strongly depends on the fraction  $\eta_{Earth}$  of targets which actually have an Earth-like planet. For the results shown in Tab. 2 we assumed that all targets searched have a planet. In this case all our formations fulfil the mission requirements. The performance of the planar and the non-planar implementation of the orthogonal TTN is comparable.

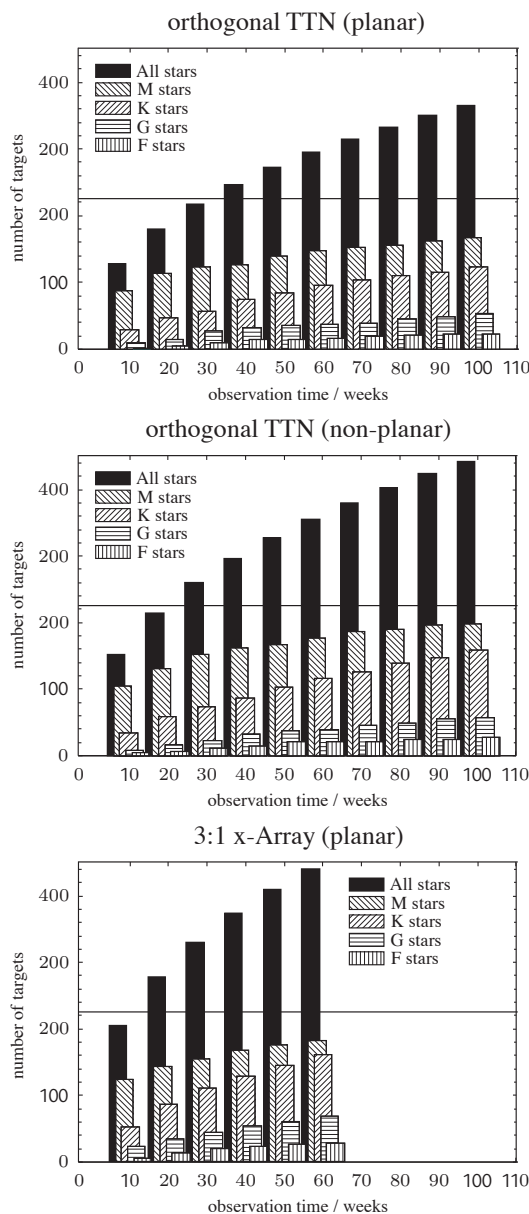


Figure 2. Number of targets searched for a planet as a function of time for promising aperture configurations, assuming an exo-zodi level similar to that of the Earth. The number of targets is given by the time required to achieve for a planet detection probability of 90% a SNR of 5 for the demodulated planet signal. Each target is visited three times to determine the orbit parameters and the observation duty cycle is 70%.

The x-Array again clearly outperforms all other configurations and therefore allows for the lowest  $\eta_{\text{Earth}}$ . For most targets, water detection at the long edge of the DARWIN wavelength range turned out to be most efficient. After a prioritization of the targets this might allow for a reduction of the observational wavelength range and therefore for a simplification of the instrument.

configuration formation	orthogonal TTN				x-Array	
	planar		non-planar		planar	
zodi level	1	10	1	10	1	10
search time	229	324	157	254	86	119
no. of planets	45	23	52	25	76	42

Table 2. Science performance with respect to target search (time required in days) and planet spectroscopy (number of planets analyzed) for promising aperture configurations. The x-Array has an imaging to nulling baseline ratio of  $X_B = 3$ . The nominal mission lifetime is 5 years, the observation duty cycle is 70%, and the spectroscopy phase starts immediately after 225 or 150 planets have been detected for 1 or 10 zodi, respectively. For the number of planets characterized we assumed that all stars searched have a planet, i.e.  $\eta_{\text{Earth}} = 1$ .

## 5. DARWIN MISSION BASELINE

By taking into account the expected science performance and the technical feasibility as well as mission and instrument complexity, cost and risk, we arrived at a baseline design for the DARWIN mission.

The x-Array aperture configuration in planar spacecraft formation clearly achieves the best science performance because it allows for the most efficient instrument implementation. The x-Array outperforms the other formations in terms of target search and especially in terms of planet spectroscopy. Even if only a small fraction of the targets searched have a planet, the x-Array promises acceptable science return. Because of the high angular resolution – which can be set independently from the nulling performance – the x-Array allows for unambiguous and reliable reconstruction which even makes the resolving of multi-planet systems possible.

The x-Array allows for the most compact and efficient design of the modulation and recombination unit. Because of the by 33% larger collecting area and because of the by 43% higher instrument efficiency the x-Array allows for a clearly higher science return. The compactness of the nulling core reduces the overall complexity and simplifies the control of tip/tilt and relative optical path differences. The x-Array has the big advantage that the critical phase shifts of  $\pi$  required for nulling can be realized by perfectly achromatic periscopes, thus minimizing the number of complex dielectric phase shifter systems which required highly accurate cryogenic mechanisms and metrology. Because of the limited launch volume the receive telescopes for the planar formations require a deployable secondary mirror. A sufficiently sta-

ble deployment mechanism appears feasible but requires some metrology for accurate alignment.

The x-Array in planar spacecraft formation relies only on well established concepts which minimizes the development risks. In contrast to this, the non-planar formations (“EMMA”) require completely new system and subsystem concepts. This imposes an incalculable high technological risk which is closely related to high development costs. Especially the testability of the collector mirrors on ground as well as the feasibility of the aberration corrector and derotation optics are considered as highly questionable. In contrast to three telescope formations, the x-Array allows for science operation even if one collector spacecraft fails. Although the science performance is reduced to 62% of that of three telescope formations, it avoids launching a spare satellite and thus reduces the overall mission costs.

The costs for planar formations with three and four telescopes are comparable. Because they are mainly driven by the development of the two different types of spacecraft and not by the number of collector spacecraft, the x-Array is by less than 10% more expensive than a planar three telescope nuller. For the non-planar formations dramatically higher costs are expected because of the incalculable high technological risks of the required new system and subsystem concepts.

Launch with a single Ariane 5 ECA is the only launch option for the DARWIN mission due to the mass and volume requirements. Direct injection into a transfer to L2 and early separation of the composite stack in LEOP allows for the desired performance but results in lowest mission complexity. The dispersion correction manoeuvres can be performed by solar electric propulsion which may also be used for all coarse formation manoeuvres as slew and resizing as well as for FDIR (fault detection isolation and recovery) and collision avoidance actions. Free insertion into a Halo orbit at L2 is preferred as it allows for simplified operations. It can be directly reached from the Kourou for half a year or requires only small insertion manoeuvres which can also be performed by solar electric propulsion.

## 6. SUMMARY AND CONCLUSION

We provided a discussion of the key mission and configuration options for the DARWIN mission and presented the results of the science performance prediction for promising spacecraft formations. We arrived at a baseline mission design by taking into account the achievable science performance and the technical feasibility as well as complexity, cost and risk.

Because of the superior science performance at marginally increased costs and because of the most compact and efficient instrument concept allowing for easiest implementation, we conclude on a mission baseline including a planar x-Array formation, directly injected by



a single Ariane 5 ECA launch vehicle into a transfer to a Halo orbit at L2, where the composite stack is separated in LEOP and solar electric propulsion is used for the correction manoeuvres. The proposed instrument relies only on well established concepts with proven feasibility.

We have shown that the DARWIN mission is feasible and that the mission requirements can be fulfilled by an optimized instrument concept. Maximum science performance can be achieved by a well established planar formation with four apertures in a x-Array configuration.

#### ACKNOWLEDGMENTS

The work described was performed under ESA/ESTEC contract AO/1-4881/05/NL/NB, *DARWIN System Assessment Study*, performed by EADS Astrium. The authors are grateful to J. Borde, S. Boulade, B. Calvel, M. Grimmer, S. Kemble, L. Maleville, A. Povoleri, L. Serafini, R. Slade, A. Villien, and R. Wall as well as to L. d'Arcio, M. Fridlund, R. den Hartog, and A. Karlsson for their contribution and assistance.

#### REFERENCES

1. European Space Agency, May 2006, available online <http://sci.esa.int/darwin>
2. Bracewell R.N. 1978, *Nature* **274**, 780–782
3. Karlsson A. Wallner O. Perdignes Armengol J. Absil O. 2004, *Proc. SPIE* **5491**, 831–841
4. Velusamy T. Angel R.P. Eatchel A. Tenerelli D. Woolf N.J. 2003, *ESA-SP* **539**
5. Lay O. Dubovitsky S. 2004, *Proc. SPIE* **5491**, 874–885
6. Kaltenecker L. Eiroa C. Stankov A. Fridlund M. 2005, *Proc. IAU* **200**, 89–92
7. Lay O.P. 2004, *Appl. Opt.* **43**, 6100–6123
8. Wallner O. Perdignes Armengol J. Karlsson A. 2004, *Proc. SPIE* **5491**, 798–805
9. Serabyn E. Colavita M.M. 2001 *Appl. Opt.* **40**, 1668–1671